Proceeding of Symposium Gyro Technology 2002, Stuttgart, Germany. pp. 2.0-2.15

Analytical Design of Coriolis Vibratory Gyroscopes

V.A. Apostolyuk

Micro and Nano Systems Cluster
Institute of Materials Research and Engineering
3 Research Link, 117602
SINGAPORE

Logeeswaran V.J., F.E.H. Tay

Department of Mechanical Engineering
National University of Singapore
10 Kent Ridge Crescent, 119260
SINGAPORE

Summary

In this paper a generalised approach to the analysis of the dynamics and errors of different types of Coriolis Vibratory Gyroscopes (CVG), as well as calculation of their performances for application in the design of such gyroscopes, is considered. In particular dynamics and errors of single mass gyroscopes, for both translational and rotational movement of the sensitive element, is investigated and analysed. Based on the generalised equations, analytical dependencies for basic errors, such as scale factor non-linearity, bias from misalignment between elastic and measurement axes, bias from vibrations and dynamic error caused by harmonic angular rate, are derived and analysed. A methodology for the optimal design of the sense element has been developed and the results applied to the design, fabrication and testing of a micromechanical CVG.

Introduction

Fabrication technologies for microcomponents, microsensors, micromachines and micro-electromechanical systems (MEMS) are being rapidly developed, and represent a major research effort worldwide. There are many techniques currently being utilised in the production of different types of MEMS including inertial micro-sensors that made it possible to fabricate MEMS in high volumes at low individual cost.

Micro-mechanical CVGs have already been proposed for or actually deployed in numerous applications, including automotive active suspension and traction control systems, air bag activation, consumer electronics, guided munitions, robotics, etc. As the technology advances, micro-mechanical sensors will be deployed in many other functions that can benefit from the inexpensive detection of angular rate as well as other motion parameters. A key component of the angular rate sensor is a mechanical structure (or sensitive element) that is sensitive to rotation. One of the main problem sources in CVG development is intuitive design approach and almost absolute absence of the well-developed operation and error theories as well as analytical design methodologies. Currently designers have to make numerous simulations and experiments trying to obtain the appropriate designs for sensitive elements. This approach only occasionally could result in an optimal and efficient design. As a result, performances of all present micro-mechanical CVG still remain very low, which significantly reduces number of the possible applications.

One of the ways to improve performances of CVG is to analyse their dynamics and errors. Mathematical models of symmetrical (without decoupling frames) sensitive elements with translational movement of a proof mass applicable to analysis of CVG were considered in [1] and [2]. Dynamics and errors of gimballed and tuning fork micro-mechanical gyroscopes were considered in [3-5]. Dynamics and errors of translation CVG with a decoupling frame were studied in [6,7]. Some calculations of performances for micro-mechanical gyroscopes with translational oscillations of a proof mass were considered in [8, 9]. But no analytical approaches to design were developed in any of the mentioned papers.

In this paper, we considered a common approach to the analysis of the dynamics and errors of different types of Coriolis vibratory gyroscopes as well as calculation of their performances for application in the design of such gyroscopes.

Angular rate sensing and motion equations of the sensitive element

For most CVGs, the sensitive element can be represented as an inertia element and elastic suspension with two degrees of freedom. The sensitive element is excited to oscillate at one of its mode with prescribed amplitude. When the sensitive element rotates about a particular body-fixed axis, the resulting Coriolis force causes the proof mass to be excited in a different resonant mode. It is obvious that information about the angular rate is contained in these different oscillations. Hereinafter excited oscillations will be referred as primary oscillations and oscillations caused by angular rate will be referred as secondary oscillations.

In general, it is possible to design gyroscopes with different types of primary and secondary oscillations. For example, a combination of translation as primary oscillations and rotation as secondary oscillations as was implemented in tuning-fork gyroscopes. However, it is typically more convenient for single-mass gyroscopes to be implemented with the same type of primary and secondary oscillations.

The dynamics of a sensitive element of Coriolis vibratory gyroscopes can be described by a set of dynamic parameters as follows: k_1, k_2 - natural frequencies of secondary and primary oscillations; ζ_1, ζ_2 - relative damping factors; ω - operating (driving) frequency.

They entirely determine structural parameters such as mass, length of springs and vacuum level among others for any achievable fabrication process. On the other hand, characteristics such as measurement range, sensitivity, resolution, bias and bandwidth are the subject of sensitive element design process. Let us determine dependencies and rules that can allow us to obtain dynamic parameters and technology tolerances on the basis of final technical requirements.

Let us introduce the right-handed orthogonal and normalized reference basis in which primary oscillations are excited along the second axis, secondary along the first axis and therefore the third axis is the sensitive axis (see fig. 1).

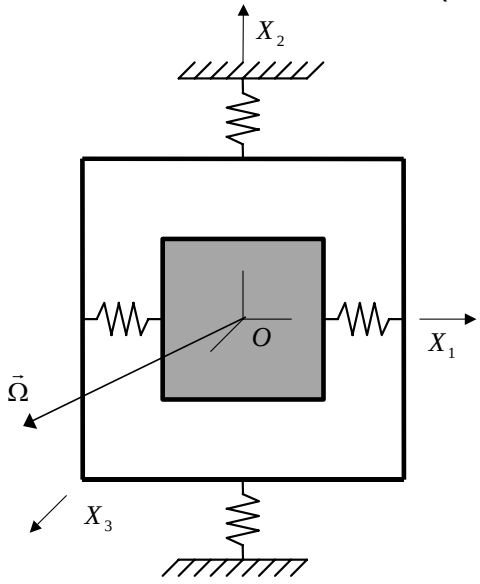

Fig. 2. Sensitive element of a single-mass CVG

Assuming that the reference basis rotates with an arbitrary angular rate vector $\vec{\Omega} = \{\Omega_1, \Omega_2, \Omega_3\}$ generalised equations of motion of a single-mass sensitive element can be presented in the form

$$\begin{cases} \ddot{x}_1 + 2\zeta_1 k_1 \dot{x}_1 + \left(k_1^2 - d_1\Omega_3^2\right)x_1 - g_1\Omega_3\dot{x}_2 = q_1(t) \\ \ddot{x}_2 + 2\zeta_2 k_2 \dot{x}_2 + \left(k_2^2 - d_2\Omega_3^2\right)x_2 + g_2\Omega_3\dot{x}_1 = q_2(t), \end{cases} \quad (1)$$

where $q_i(t)$ represents either force/mass or torque/inertia about the corresponding axis and x_i represents either translation or angular displacements of the proof mass. Other factors introduced in (1) are given in Table 1. In Table 1, all moments of inertia are presented in the form I_{ij} where the first index refers to the variable x while the second index refers to the axis.

Table 1. Dimensionless inertia parameters

	Translational	Rotational
d_1	1	$(I_{12}-I_{13})/I_{11}$
d_2	1	$(I_{21}-I_{23})/I_{22}$
g_1	2	$(I_{11}+I_{12}-I_{13})/I_{11}$
g_2	$2m_1/(m_1+m_2)$	$(I_{11}+I_{12}-I_{13})/I_{22}$

By means of equations (1) we can study dynamics of both translational and rotational sensitive elements. All parameters of inertia presented in Table 1 are subjected to the design process. Let us note that the rotational sensitive elements are more liable to be adjusted by optimisation ([10]).

Motion of a sensitive element on rotating base

Assuming an open-loop operation of the gyroscope and zero phase displacement for excitation force we can represent the right-hand part of (1) as follows:

$$q_1(t)=0,\ q_2(t)=\mathrm{Re}\{q_2\,\mathrm{e}^{i\omega t}\}. \tag{2}$$

We can also represent our generalized variables as

$$x_1(t)=\mathrm{Re}\{\overline{A}_1\,\mathrm{e}^{i\omega t}\},\ \ \overline{A}_1=A_1\,\mathrm{e}^{i\varphi_1},\ x_2(t)=\mathrm{Re}\{\overline{A}_2\,\mathrm{e}^{i\omega t}\},\ \ \overline{A}_2=A_2\,\mathrm{e}^{i\varphi_2}, \tag{3}$$

where A_1 and A_2 are the amplitudes and φ_1 and φ_2 are the phases of secondary and primary oscillations respectively. Using (2) and (3), a complex solution of the equations (1) can be obtained

$$\begin{aligned}&\overline{A}_1=\frac{g_1q_2i\omega}{\overline{\Delta}}\Omega_3,\ \overline{A}_2=\frac{q_2\left(k_1^2-d_1\Omega_3^2-\omega^2+2\zeta_1k_1i\omega\right)}{\overline{\Delta}},\\ &\overline{\Delta}=\left(k_1^2-d_1\Omega_3^2-\omega^2\right)\left(k_2^2-d_2\Omega_3^2-\omega^2\right)-\omega^2\left(4\zeta_1\zeta_2k_1k_2+g_1g_2\Omega_3^2\right)+\\ &+2i\omega\left[k_1\zeta_1\left(k_2^2-d_2\Omega_3^2-\omega^2\right)+k_2\zeta_2\left(k_1^2-d_1\Omega_3^2-\omega^2\right)\right]\end{aligned} \tag{4}$$

From (4), we can easily obtain real amplitudes of primary and secondary oscillations

$$\begin{aligned}&A_1=\frac{g_1q_2\omega}{\Delta}\Omega_3,\ A_2=\frac{q_2\sqrt{\left(k_1^2-d_1\Omega_3^2-\omega^2\right)^2+4k_1^2\zeta_1^2\omega^2}}{\Delta},\\ &\Delta^2=\left[\left(k_1^2-d_1\Omega_3^2-\omega^2\right)\left(k_2^2-d_2\Omega_3^2-\omega^2\right)-\omega^2\left(4\zeta_1\zeta_2k_1k_2+g_1g_2\Omega_3^2\right)\right]^2+\\ &+4\omega^2\left[k_1\zeta_1\left(k_2^2-d_2\Omega_3^2-\omega^2\right)+k_2\zeta_2\left(k_1^2-d_1\Omega_3^2-\omega^2\right)\right]^2\end{aligned} \tag{5}$$

and also their phases given by

$$\begin{aligned}&\mathrm{tg}(\varphi_1)=\frac{\left(k_1^2-d_1\Omega_3^2-\omega^2\right)\left(k_2^2-d_2\Omega_3^2-\omega^2\right)-\omega^2\left(4\zeta_1\zeta_2k_1k_2+g_1g_2\Omega_3^2\right)}{2\omega\left[k_1\zeta_1\left(k_2^2-d_2\Omega_3^2-\omega^2\right)+k_2\zeta_2\left(k_1^2-d_1\Omega_3^2-\omega^2\right)\right]},\\ &\mathrm{tg}(\varphi_2)=\frac{2\omega\left[\left(k_1^2-d_1\Omega_3^2-\omega^2\right)b_1+k_1\zeta_1b_2\right]}{\left(k_1^2-d_1\Omega_3^2-\omega^2\right)b_2-4k_1\zeta_1\omega^2b_1},\\ &b_1=k_1\zeta_1\left(k_2^2-d_2\Omega_3^2-\omega^2\right)+k_2\zeta_2\left(k_1^2-d_1\Omega_3^2-\omega^2\right),\\ &b_2=\left(k_1^2-d_1\Omega_3^2-\omega^2\right)\left(k_2^2-d_2\Omega_3^2-\omega^2\right)-\omega^2\left(4\zeta_1\zeta_2k_1k_2+g_1g_2\Omega_3^2\right).\end{aligned} \tag{6}$$

Using formulae (5) and (6) for the amplitudes and phases respectively, we can determine the sensitivity of a single mass Coriolis vibratory gyroscope.

Sensitivity and linearity

As follows from (5), the amplitude of secondary oscillations depends on the angular rate Ω_3. Let us represent this amplitude by dimensionless variables by means of the following substitution

$$k_1 = k\delta k\ ,\ k_2 = k\ ,\ \omega = k\delta\omega\ ,\ \Omega_3 = k\delta\Omega\ , \tag{7}$$

as a function of new dimensionless variable amplitude given by

$$\begin{aligned} A_1 &= \frac{g_1 q_2 \delta\omega}{k^2 \Delta}\delta\Omega\ , \\ \Delta^2 &= \left[\left(\delta k^2 - d_1\delta\Omega^2 - \delta\omega^2\right)\left(1 - d_2\delta\Omega^2 - \delta\omega^2\right) - \delta\omega^2\left(4\delta k\zeta_1\zeta_2 + g_1 g_2\delta\Omega^2\right)\right]^2 + \\ &+ 4\delta\omega^2\left[\delta k\zeta_1\left(1 - d_2\delta\Omega^2 - \delta\omega^2\right) + \zeta_2\left(\delta k^2 - d_1\delta\Omega^2 - \delta\omega^2\right)\right]^2 \end{aligned} \tag{8}$$

Note that no assumption on the value of the angular rate was made. It is obvious that the relationship between the amplitude of the secondary oscillations and the angular rate is not linear. However, for the optimal performance this dependence has to be linear. The sensitivity can be taken as the gradient of dependence (8) at the origin. In this case sensitivity for the relative angular rate $\delta\Omega$ can be given by

$$C_\Omega = \frac{g_1 q_2 \delta\omega}{k^3\sqrt{\left(\left(\delta k^2 - \delta\omega^2\right)^2 + 4\delta k^2\delta\omega^2\zeta_1^2\right)\left(\left(1 - \delta\omega^2\right)^2 + 4\delta\omega^2\zeta_2^2\right)}}\ , \tag{9}$$

where $A_{10} = C_\Omega\Omega$ is the desirable output as compared with A_1. The dependence of the sensitivity on the natural frequencies ratio δk and drive frequency $\delta\omega$ is shown in Fig. 2.

Analysis of Fig. 2 shows that the biggest sensitivity is achievable only if natural frequencies are equal and excitation occurs on the eigenfrequency of primary oscillations. Moreover, considering (9) it is apparent that for better sensitivity the natural frequency of primary oscillations has to be as low as possible.

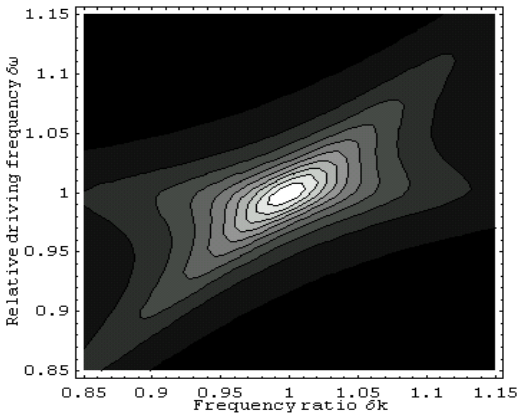

Fig. 2. Sensitivity as a function of natural frequency ratio δk and relative driving frequency $\delta\omega$

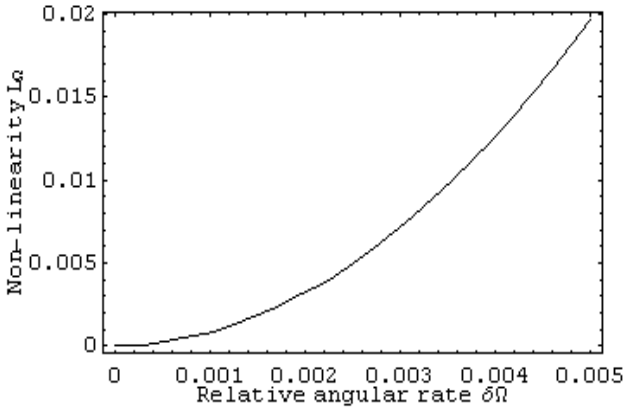

Fig. 3. Non-linearity as a function of the relative angular rate

On the other hand it will lead us to the non-linear angular rate transformation. Let us introduce a non-linearity dimensionless parameter as

$$L_\Omega = 1 - \frac{A_1}{A_{10}}\ .$$

The relationship between L_Ω and the angular rate $\delta\Omega$ is shown in fig. 3. For given small values of non-linearity $L_\Omega < 0.05$ we can obtain following the approximate formula for relative angular rate

$$\delta\Omega^* = \left\{ \frac{L_\Omega \left[\left(\delta k^2 - \delta\omega^2\right)^2 + 4\delta k^2 \delta\omega^2 \zeta_1^2 \right] \left[\left(1 - \delta\omega^2\right)^2 + 4\delta\omega^2 \zeta_2^2 \right]}{\left(\delta\omega^2 - 1\right) D_0 + 4\delta\omega^2 \left[g_1 g_2 \delta k \delta\omega^2 \zeta_1 \zeta_2 - d_1 \zeta_2^2 \left(\delta k^2 - \delta\omega^2\right) \right]} \right\}^{\frac{1}{2}}, \tag{10}$$

where $D_0 = \left(\delta k^2 - \delta\omega^2\right)\left(d_1 + d_2 \delta k^2 - \left(d_1 + d_2 - g_1 g_2\right)\delta\omega^2\right) + 4 d_2 \delta k^2 \delta\omega^2 \zeta_1^2$. Assuming a value for L_Ω and a suitable measurement range of the angular rate $\Omega_{\max}$, $\delta\Omega^*$ can be obtained from (10). From (7), we can then calculate the minimal value for the natural frequency of primary oscillations

$$k_{\min} = \frac{\Omega_{\max}}{\delta\Omega^*}. \tag{11}$$

For example, if $L_\Omega = 0.01$ and $\Omega_{\max} = 1.0\, s^{-1}$ then minimal value for the natural frequency of primary oscillations will be $k_{\min} \approx 45\,\mathrm{Hz}$. Such a low value for the frequency means that the lower limit will in fact be determined by other factors but nevertheless there is no reason to make it very high.

Resolution

Formulae for calculation of resolution for the single mass CVG can be obtained by means of given minimal capacity changes, which the device is capable of detecting. Let us denote this minimal change as $\Delta C_{\min}$. In case of differential measurement the resulting capacitance change is produced by the subtraction of two separately measured capacitances C_1 and C_2 as follows:

$$\Delta C(\delta) = C_1(\delta) - C_2(\delta) \approx 2 \frac{dC(0)}{d\delta} \delta, \tag{12}$$

where δ is the displacement of the electrodes. The shift of the electrodes caused by changes of the angular rate $\Delta\Omega$ is given by

$$\delta = r_0 C_\Omega \Delta\Omega, \tag{13}$$

where C_Ω is determined by (9), r_0 is the distance from the rotation axis to the centre of electrode for the rotary sensitive element and unity for the translational sensitive element. Thus, comparing (12) and (13), we can obtain the resolution of a single mass Coriolis vibratory gyroscope that is given by

$$\Delta\Omega_{\min} = \frac{\Delta C_{\min} k^3 \sqrt{\left(\left(\delta k^2 - \delta\omega^2\right)^2 + 4\delta k^2 \delta\omega^2 \zeta_1^2\right)\left(\left(1 - \delta\omega^2\right)^2 + 4\delta\omega^2 \zeta_2^2\right)}}{2 \frac{dC(0)}{d\delta} r_0 g_1 q_2 \delta\omega} \tag{14}$$

Note that formula (14) represents the resolution with a capacitive readout. However, the same procedure can be applied to any readout principle. The best resolution corresponds to a minimal $\Delta\Omega_{\min}$.

Bias

Bias in CVGs can be the result of many different factors. Let us consider sources of bias concerned with the sensitive element and its dynamics. One of them is vibration at the drive frequency. Interference of vibrations at other frequencies can be filtered. It is obvious that for the translational gyroscopes, only translational vibration will have an effect and for rotational gyroscopes, only angular vibrations will be

relevant. Therefore, in the case of vibrations at drive frequency, the motion equations of the sensitive element will be

$$\begin{cases} \ddot{x}_1 + 2\zeta_1 k_1 \dot{x}_1 + \left(k_1^2 - d_1\Omega_3^2\right)x_1 - g_1\Omega_3\dot{x}_2 = w_1(t), \\ \ddot{x}_2 + 2\zeta_2 k_2 \dot{x}_2 + \left(k_2^2 - d_2\Omega_3^2\right)x_2 + g_2\Omega_3\dot{x}_1 = q_2(t) + w_2(t). \end{cases}$$

Representing the vibrations as $w_i = w_{i0}\cos(\omega t)$, we can obtain the solution of the amplitude of secondary oscillations in relative form

$$A_{W1} = \frac{g_1 q_2 \delta\omega\delta\Omega + \sqrt{w_{10}^2\left(1-\delta\Omega^2-\delta\omega^2\right)^2 + \delta\omega^2\left(2\zeta_2 w_{10} + g_1\delta\Omega w_{20}\right)^2}}{k^2\Delta}. \tag{15}$$

If we denote the amplitude without vibrations as A_{10}, which is given by (8), then the relative error caused by vibration at drive frequency is given by

$$\delta A_W = \frac{A_{W1} - A_{10}}{A_{10}} = \frac{\sqrt{w_{10}^2\left(1-d_2\delta\Omega^2-\delta\omega^2\right)^2 + \delta\omega^2\left(2\zeta_2 w_{10} + g_1\delta\Omega w_{20}\right)^2}}{g_1 q_2 \delta\omega\delta\Omega} \tag{16}$$

Let us note that the error arising from vibration does not depend on the ratio between the natural frequencies but depends on the relative drive frequency. This dependency is shown in fig. 4.

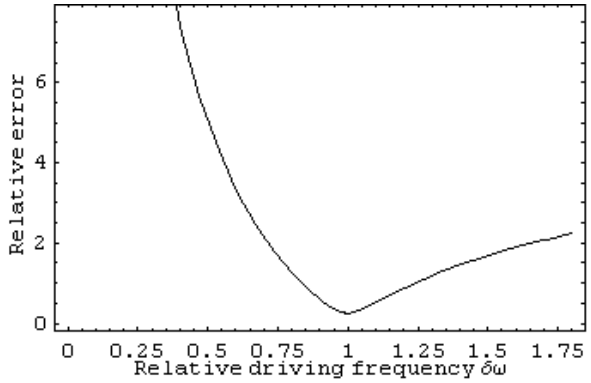

Fig. 4. Typical error from vibrations as a function of relative driving frequency

It can be easily proved that the minimal value for this error achievable at driving frequency is a solution of the following equation:

$$1 - \delta\omega^2 - d_1\delta\Omega^2 = 0 \Rightarrow \delta\omega = \sqrt{1 - d_1\delta\Omega^2} \approx 1. \tag{17}$$

This result also proves that it is preferable to drive the primary oscillations at resonance.

Another source of bias is a misalignment between elastic and readout axes. Also this error is usually referenced as quadrature error. This is most typical for the translation sensitive elements. The linearized motion equations in this case will be as follows

$$\begin{cases} \ddot{x}_1 + 2\zeta_1 k_1 \dot{x}_1 + \left(k_1^2 - d_1\Omega^2\right)x_1 - g_1\Omega\dot{x}_2 + 2\theta\Delta k_1^2 x_2 = 0, \\ \ddot{x}_2 + 2\zeta_2 k_2 \dot{x}_2 + \left(k_2^2 - d_2\Omega^2\right)x_2 + g_2\Omega\dot{x}_1 - 2\theta\Delta k_2^2 x_1 = q_2(t). \end{cases} \tag{18}$$

Here θ is the misalignment angle, $\Delta k_1^2 = \left(k_{11}^2 - k_{21}^2\right)/2$, $\Delta k_2^2 = \left(k_{22}^2 - k_{12}^2\right)/2$ and k_{ij} are the frequencies such that $k_1^2 = \left(k_{11}^2 + k_{21}^2\right)/2$ and $k_2^2 = \left(k_{22}^2 + k_{12}^2\right)/2$. The amplitude of the secondary oscillations in this case will be

$$A_1 = \frac{q_2\sqrt{g_1^2\delta\omega^2\delta\Omega^2 + 4\theta^2\delta\Delta k_1^4}}{k^2\Delta_\theta}, \tag{19}$$

$$\Delta_\theta^2 = \left[\left(\delta k^2 - d_1\delta\Omega^2 - \delta\omega^2\right)\left(1 - d_2\delta\Omega^2 - \delta\omega^2\right) - \delta\omega^2\left(4\delta k\zeta_1\zeta_2 + g_1 g_2\delta\Omega^2\right)\right]^2 +$$
$$+ 4\delta\omega^2\left[\delta k\zeta_1\left(1 - d_2\delta\Omega^2 - \delta\omega^2\right) + \zeta_2\left(\delta k^2 - d_1\delta\Omega^2 - \delta\omega^2\right) - 2\delta\Omega\theta\left(\delta\Delta k_1^2 + \delta\Delta k_2^2\right)\right]^2$$

It is obvious that if $\theta = 0$ then there is no error arising from misalignment. Moreover, this error will also be absent in the following case

$$\Delta k_1^2 = \frac{c_1 - c_2}{2m_1} = 0 \Rightarrow c_1 = c_2 . \tag{20}$$

Here c_i are the stiffness factors of the elastic suspension and m_1 is the effective mass of secondary oscillations. In addition, we can represent the amplitude (19) as a sum of two components, namely, one arising from the angular rate and the other caused by misalignment $A_1 \approx A_{10} + A_\theta$. In this case we can determine the relative error from such misalignment as

$$\delta A_\theta = \frac{A_\theta}{A_{10}} = \frac{\theta^2\delta\Delta k_1^4}{g_1\delta\omega^2\delta\Omega^2}, \ (\Omega \neq 0). \tag{21}$$

On the other hand, we can find an acceptable tolerance for the misalignment $\theta_{\max}$ assuming an acceptable relative bias $\delta\Omega_{\max}$ and condition of no rotation

$$\theta_{\max} = \frac{\delta\Omega_{\max}\delta\omega}{\delta\Delta k_1^2} . \tag{22}$$

Formula (22) also gives us an angle of misalignment if bias is known. This value can also be used for algorithmic bias compensation. If we can obtain information from other sources of primary information then it is also possible to use (19) to determine the bias compensation.

Dynamic error and bandwidth

Let us consider movement of the sensitive element on a basis that rotates with harmonic angular rate $\Omega = \Omega_0\cos(\lambda t) = \mathrm{Re}\left\{\Omega_0\, e^{i\lambda t}\right\}$. The corresponding motion equations of the sensitive element in this case, taking into account the assumption that the frequency of angular rate is small compared to the operation frequency, are given by

$$\begin{cases} \ddot{x}_1 + 2\zeta_1 k_1\dot{x}_1 + \left(k_1^2 - d_1\Omega^2\right)x_1 = g_1\Omega\dot{x}_2 + \dot{\Omega}x_2, \\ \ddot{x}_2 + 2\zeta_2 k_2\dot{x}_2 + \left(k_2^2 - d_2\Omega^2\right)x_2 = q_2\cos(\omega t) - g_2\Omega\dot{x}_1 - d_3\dot{\Omega}x_1. \end{cases} \tag{23}$$

When the amplitude of the angular rate is small ($\Omega_0 << k_2$), we can neglect the right-hand terms in the second equation of (23) except for the excitation term. In addition, centrifugal accelerations in this case are small and hence the equations reduce to

$$\begin{cases} \ddot{x}_1 + 2\zeta_1 k_1\dot{x}_1 + k_1^2 x_1 = g_1\Omega\dot{x}_2 + \dot{\Omega}x_2, \\ \ddot{x}_2 + 2\zeta_2 k_2\dot{x}_2 + k_2^2 x_2 = q_2\cos(\omega t). \end{cases} \tag{24}$$

Partial solution of the second equation in (24) is given by the following

$$x_2(t) = \mathrm{Re}\left\{\overline{A}_2\, e^{i\omega t}\right\} = \mathrm{Re}\left\{A_2\, e^{i(\omega t + \varphi_2)}\right\},$$

$$A_2 = \frac{q_2}{k^2\sqrt{\left(1 - \delta\omega^2\right)^2 + 4\zeta_2^2\delta\omega^2}}, \ \mathrm{tg}(\varphi_2) = -\frac{2\zeta_2\delta\omega}{1 - \delta\omega^2} .$$

Then, the right-hand part of the first equation in (24) will be

$$-\frac{\Omega_0}{2}\mathrm{Im}\left\{\overline{A}_2\left(g_1\omega + \lambda\right)e^{if_1 t} + \overline{A}_2\left(g_1\omega - \lambda\right)e^{if_2 t}\right\}, \ f_{1,2} = \omega \pm \lambda .$$

Partial solution of (24) for the secondary oscillations x_1 yields a solution given by a sum of two oscillations with frequencies $f_{1,2} = \omega \pm \lambda$:

$$x_1(t) = \mathrm{Im}\left\{\overline{A}_{11}\, e^{if_1 t} + \overline{A}_{12}\, e^{if_2 t}\right\}.$$

After substitution of the supposed solution in the first equation of (24) we can find complex amplitudes of secondary oscillations

$$\overline{A}_{11,12} = -\frac{\Omega_0 q_2 (g_1 \delta\omega \pm \delta\lambda)}{2k^3\left[\delta k^2 - (\delta\omega \pm \delta\lambda)^2 + 2\zeta_1 \delta k i(\delta\omega \pm \delta\lambda)\right]\left[1 - \delta\omega^2 + 2\zeta_2 i\delta\omega\right]},$$

where $\delta\lambda = \lambda/k$ is the relative frequency of the angular rate. Transition to real amplitude and phase gives us

$$A_{11,12} = \frac{\Omega_0 q_2 (g_1 \delta\omega \pm \delta\lambda)}{2k^3\sqrt{\left\{\left[\delta k^2 - (\delta\omega \pm \delta\lambda)^2\right]^2 + 4\zeta_1^2 \delta k^2 (\delta\omega \pm \delta\lambda)^2\right\}\left\{(1 - \delta\omega^2)^2 + 4\zeta_2^2 \delta\omega^2\right\}}}.$$

Hence the partial solution for the secondary oscillations is given by

$$x_1(t) = A_{11}\sin\left[(\omega + \lambda)t + \varphi_{11}\right] + A_{12}\sin\left[(\omega - \lambda)t + \varphi_{12}\right]. \qquad (25)$$

Here the phase shifts $\varphi_{11,12}$ are determined from the following expression

$$tg(\varphi_{11}) = 2\frac{\delta\omega\zeta_2\left(\delta k^2 - (\delta\lambda + \delta\omega)^2\right) + \delta k\zeta_1(1 - \delta\omega^2)(\delta\omega + \delta\lambda)}{4\delta k\delta\omega\zeta_1\zeta_2(\delta\lambda + \delta\omega) - (1 - \delta\omega^2)\left(\delta k^2 - (\delta\omega + \delta\lambda)^2\right)},$$

$$tg(\varphi_{12}) = 2\frac{\delta\omega\zeta_2\left(\delta k^2 - (\delta\omega - \delta\lambda)^2\right) + \delta k\zeta_1(1 - \delta\omega^2)(\delta\omega - \delta\lambda)}{4\delta k\delta\omega\zeta_1\zeta_2(\delta\omega - \delta\lambda) - (1 - \delta\omega^2)\left(\delta k^2 - (\delta\omega - \delta\lambda)^2\right)}.$$

Assuming that $\Omega = const \Rightarrow \delta\lambda = 0$, we can obtain the amplitude and phase of the secondary oscillations when the angular rate is constant. By making the following substitutions: $A_{11,12} = A_{10}(1 \pm \delta A)$, $\varphi_{11,12} = \varphi_0 \pm \Delta\varphi$, the solution (25) will change to

$$x_1(t) = 2A_{10}\left[\cos(\lambda t + \Delta\varphi)\sin(\omega t + \varphi_0) + \delta A\sin(\lambda t + \Delta\varphi)\cos(\omega t + \varphi_0)\right].$$

After multiplying signal corresponding to the secondary oscillations on a carrier signal $\sin(\omega t + \varphi_0)$, the output will be as follows

$$x_1^*(t) = A_{10}\left[\cos(\lambda t + \Delta\varphi) - \cos(\lambda t + \Delta\varphi)\cos(2\omega t + 2\varphi_0) + \right.$$
$$\left. + \delta A\sin(\lambda t + \Delta\varphi)\sin(2\omega t + 2\varphi_0)\right].$$

The first item $A_{10}\cos(\lambda t + \Delta\varphi)$ is the signal proportional to the angular rate. All other items have doubled frequency and must be removed by filtering after demodulation. The output signal is distorted both in amplitude and phase. Phase distortion $\Delta\varphi$ is well predictable in a very wide range by means of obtained formulae. Amplitude error caused by the harmonic angular rate is

$$\delta\Omega = \frac{A_{10} - A_0}{A_0} \approx K_\lambda \delta\lambda^2, \qquad (26)$$

where

$$K_\lambda = \frac{\delta\omega^6(3g_1 - 2) + h\delta k^2\left[\delta k^4(2 + g_1) - \delta\omega^4(5g_1 - 6)\right] + \delta k^4\delta\omega^2\left[4h^2(g_1 - 1) - 2 - 3g_1\right]}{g_1\left[\left(\delta k^4 + \delta\omega^4 - 2\delta k^2\delta\omega^2 h\right)\right]^2},$$

$$h = 1 - 2\zeta_1^2,\ A_0 = A_{10}(\delta\lambda = 0).$$

Formula (26) gives only approximate results but for small values of the relative frequency of the angular rate ($\delta\lambda < 0.01$) they are acceptable. The exact formula is more complex and there is no reason to use it in this context. Graphs corresponding to both approximate and exact dependence are shown in fig. 5. It is apparent that the dynamic error increases if the ratio between the natural frequencies approaches

unity. In addition, it is possible to calculate a bandwidth if one assumes an acceptable relative dynamic error $\delta\Omega_{\max}$

$$B_\Omega = k\sqrt{\frac{\delta\Omega_{\max}}{K_\lambda}}. \tag{27}$$

Here, the bandwidth B_Ω is measured in radians per second. The graph for the bandwidth is shown in fig. 6.

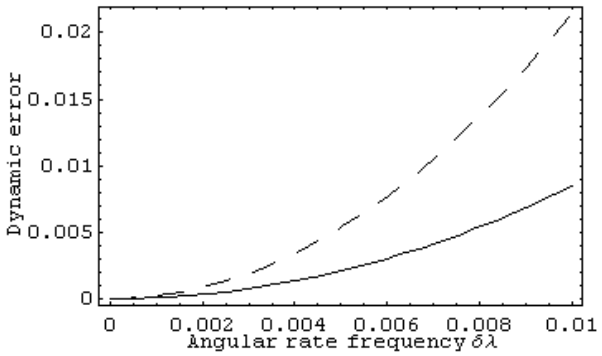

Fig. 5. Dynamic error as a function of relative angular rate frequency (dashed line $\delta k = 1.05$, solid line $\delta k = 1.1$)

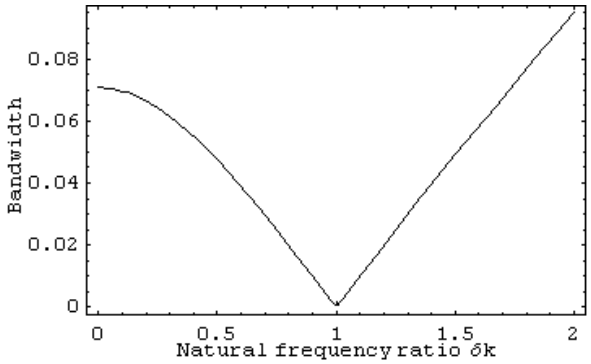

Fig. 6. Relative bandwidth as a function of ratio of the natural frequencies ($\delta\Omega_{\max} = 0.01$)

Analyzing both fig. 6 and fig. 2, we can see that as the ratio of the natural frequencies approaches unity (i.e. $\delta k \approx 1$), one will obtain the maximal sensitivity but the minimal bandwidth. This effectively leads to a trade-off between these parameters. For open-loop gyroscopes, it is acceptable to have a ratio of the natural frequencies in the range of 0.9 – 0.95. For closed-loop operation, it is reasonable to have a ratio $\delta k \approx 1$ for maximal sensitivity but providing necessary bandwidth by feedback.

Design methodology

The presented analysis of the sensitivity, linearity and bandwidth has resulted in two main design trade-offs. First, in order to increase sensitivity, operational frequencies have to be as low as possible, but at the same time there is a lower limit that depends on scale factor linearity requirements. As a result, the natural frequency of the primary oscillations can be chosen by means of formula (11) taking into consideration acceptable value of the non-linearity and required measurement range. Second, in order to obtain maximum sensitivity, both natural frequencies of primary and secondary oscillations have to be of the same value, but it will result in a minimum for the bandwidth. This trade-off can be resolved by formula (27) so that the ratio of the natural frequencies can be designed to provide the necessary bandwidth. As a result, such parameters as driving frequency, primary natural frequency (natural frequency of the primary oscillations) and ration of the natural frequency can be directly calculated and they have to be precisely implemented during sensitive element design.

Testing results

Presented design methodology was used in designing of a micro-mechanical CVG. In order to make design process efficient specialised design software tool was developed. Based on the formulae presented in the paper the software allows not only real-time observation of the mechanical parameters of the sensitive element but

also all the main gyroscope performances during design process. After finishing of the design, geometry of the sensitive element can be exported directly to the mask file. Details of the in-house developed software are available from the authors. Some photos of the fabricated sensitive element are shown in Figures 7 and 8.

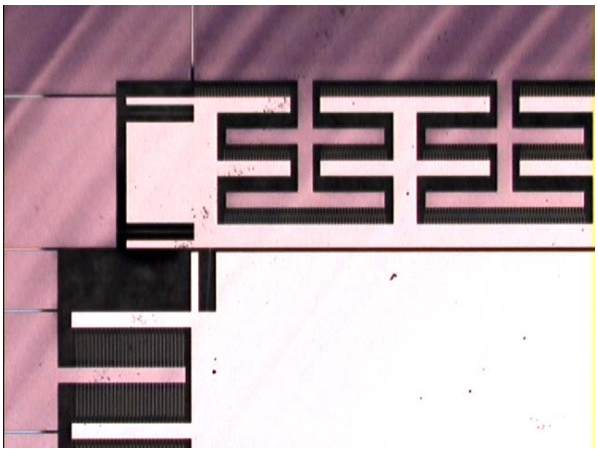

Fig. 7. Part of the sensitive element

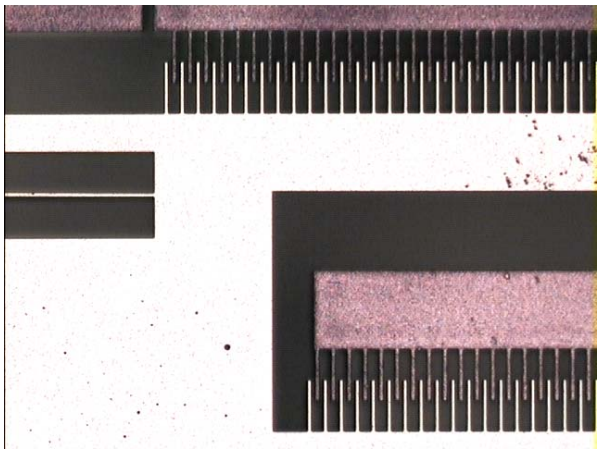

Fig. 8. Driving comb-structures

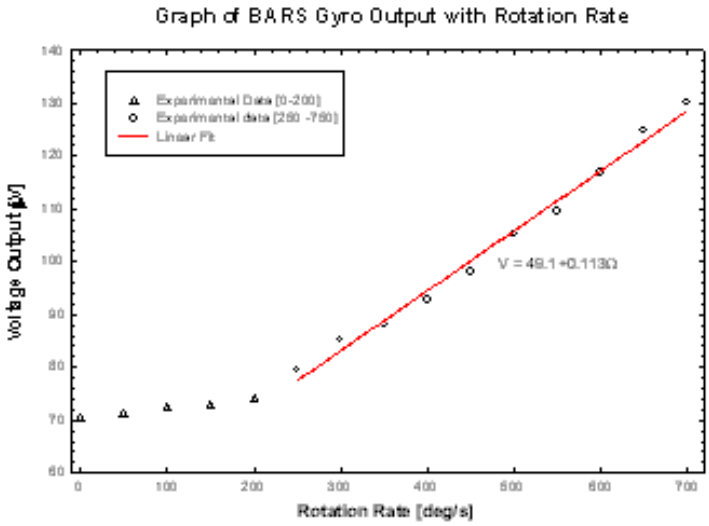

Fig. 9. Gyroscope rate testing results

Rate table tests of the fabricated micro-mechanical gyroscope were conducted and results are shown in Figure 9. Note that the gyroscope was tested in the air (no vacuum) as well as without on-chip electronics, which resulted in significant measurement noise. Due to the low natural frequency and optimal design, sensitivity to the angular rate nevertheless was indeed detected. Low level and non-linearity of the response for the small angular rate is caused by the measurement noise.

Conclusion

The presented analytical approach to the design of the sensitive element of Coriolis vibratory gyroscopes allows both prediction of the performances and determination of the design parameters that are necessary to achieve high performance of inertial instruments. Even though the proposed approach is applied to sensitive elements, most of the dependencies can also be used for detailed analysis of the dynamics of CVGs while designing control circuits. Due to the optimal design, the sensitivity to the angular rate was detected even without vacuum packaging and low-noise on-chip application specific integrated circuits.

Acknowledgement

We would like to appreciate the assistance of Mr. Tang Xiaosong and Ms. Chan Mei Lin in fabrication and testing of the gyroscope. The first author is grateful to the department of Inertial Sensors and Control Systems of Flying Vehicles of the Aero-Space Systems Faculty in the National Technical University of Ukraine "Kiev Polytechnic Institute" and personally to Prof. Alexander Zbrutsky for useful discussions on earlier stages of this work.

References

[1] Friedland, B., Hutton, M. F., "Theory and Error Analysis of Vibrating-Member Gyroscope," IEEE Transactions on Automatic Control, vol. AC-23, 1978, no. 4, pp. 545-556.

[2] Lynch, D., "Vibratory Gyro Analysis by the Method of Averaging," Proceedings of 2nd St. Petersburg Conf. on Gyroscopic Technology and Navigation, St. Petersburg, 1995, pp.26-34.

[3] Apostolyuk, V., Zbrutsky, A., "Investigation of Micromechanical Inertial Devices," Proceedings of 4-th St. Petersburg International Conference on Integrated Navigation Systems, St. Petersburg, 1997, pp. 330-336.

[4] Apostolyuk, V., Zbrutsky, A., "Investigation of dynamics of a gimballed micro-mechanical gyroscope," Journal "Scientific news of the National Technical University of Ukraine", Kiev, 1998, No. 3, pp. 115-121.

[5] Apostolyuk V., Zbrutsky, A., "Thermal errors of gimballed micromechanical gyroscopes", Journal "Mechanics of gyroscopic systems," Kiev, 2000, No. 5-16, pp. 3-10.

[6] Apostolyuk, V., Zbrutsky, A., "Dynamics of a sensitive element of the micromechanical gyroscopes with an additional frame", Journal "Gyroscopes and Navigation", St. Petersburg, 1998, No. 3 (22), pp. 13-23.

[7] Apostolyuk, V., Zbrutsky, A., "Dynamics of a sensitive element of micromechanical gyroscope" Journal "Scientific news of the National Technical University of Ukraine", Kiev, 1999, No 1, pp. 114-120.

[8] Geiger, W., Folkmer, B., Sobe, U., Sandmaier, H., Lang, W., "New designs of Micromachined vibrating rate gyroscopes with decoupled oscillation modes," Sensors and Actuators A66, 1998, pp. 118-124.

[9] Apostolyuk, V., Zbrutsky, A., "Comparative analysis of the performances of micromechanical gyroscopes with translation and angular motions of sensitive elements", Journal "Gyroscopes and Navigation", St. Petersburg, No 1, 2000, pp. 22-34.

[10] Apostolyuk, V., Zbrutsky, A., "Sensitive element's structure optimisation for gimballed micromechanical gyroscopes", Journal "Mechanics of gyroscopic systems", Kiev, 2000, No. 5 -16, pp. 11-19.